Solid-State DNA Sizing by Atomic Force Microscopy

ARTICLE *in* ANALYTICAL CHEMISTRY · JUNE 1998

Impact Factor: 5.64 · DOI: 10.1021/ac971187o · Source: PubMed

7 AUTHORS, INCLUDING:

Ye Fang
Corning Incorporated
131 PUBLICATIONS **3,404** CITATIONS
SEE PROFILE

Tim Wiltshire
University of North Carolina at Chapel Hill
110 PUBLICATIONS **8,404** CITATIONS
SEE PROFILE

Roger H Reeves
Johns Hopkins University
170 PUBLICATIONS **7,040** CITATIONS
SEE PROFILE

Anal. Chem. **1998,** *70,* 2123−2129

Solid-State DNA Sizing by Atomic Force Microscopy

Ye Fang,[†] Thomas S. Spisz,[‡] Tim Wiltshire,[†] Neill P. D'Costa,[†] Isaac N. Bankman,[‡] Roger H. Reeves,[†] and Jan H. Hoh*[,†]

Department of Physiology, Johns Hopkins University School of Medicine, 725 North Wolfe Street, Baltimore, Maryland 21205 and Applied Physics Laboratory, Johns Hopkins University, Johns Hopkins Road, Laurel, Maryland 20723

Atomic force microscopy (AFM) allows rapid, accurate, and reproducible visualization of DNA adsorbed onto solid supports. The images reflect the lengths of the DNA molecules in the sample. Here we propose a solid-state DNA sizing (SSDS) method based on AFM as an analytical method for high-throughput applications such as fingerprinting, restriction mapping, +/− screening, and genotyping. For this process, the sample is first deposited onto a solid support by adsorption from solution. It is then dried and imaged under ambient conditions by AFM. The resulting images are subjected to automated determination of the lengths of the DNA molecules on the surface. The result is a histogram of sizes that is similar to densitometric scans of DNA samples separated on gels. A direct comparison of SSDS with agarose gel electrophoresis for +/− screening shows that it produces equivalent results. Advantages of SSDS include reduced sample size (i.e., lower reagent costs), rapid analysis of single samples, and potential for full automation using available technology. The high sensitivity of the method also allows the number of polymerase chain reaction cycles to be reduced to 15 or less. Because the high signal-to-noise ratio of the AFM allows for direct visualization of DNA-binding proteins, different DNA conformations, restriction enzymes, and other DNA modifications, there is potential for dramatically improving the information content in this type of analysis.

The sizing of DNA molecules is one of the most widely used analytical approaches in molecular biology and biochemistry. DNA molecules of specific lengths can be generated in many ways, such as by synthesis of complementary strands from a template DNA, digestion of DNA with restriction endonucleases, and polymerase chain reaction (PCR) amplification of a portion of a DNA molecule. The lengths of the DNA molecules are used to map distribution of restriction endonuclease recognition sites (i.e., restriction mapping), identify the presence or absence of an amplifiable target sequence (+/− screening), determine DNA sequence, establish genotypes, etc. Most DNA sizing today is performed by gel electrophoresis. By combining the appropriate gel type, gel dimensions, and applied electric field, gel electrophoresis can be used to size DNA molecules with an extensive range of molecular weights.[1] This method is relatively simple, the equipment needed inexpensive, and the results widely understood and accepted. Hence, for laboratory research, this method is useful. However, there is an increasing need for rapid, high-throughput, and inexpensive sizing methods driven by the developing field of genomics and clinical diagnostics (including genotyping). To address this need, several novel approaches to DNA sizing are being explored, including optical microscopy,[2−5] mass spectroscopy,[6−8] flow cytometry,[9,10] and electrochemistry.[11] These approaches all have potential advantages and disadvantages compared with gel electrophoresis.

Atomic force microscopy (AFM)[12] is an emerging technology that can be used for sizing of DNA adsorbed to a surface. The measured contour length determined from AFM images corresponds to the length of the DNA, as defined by the number of base pairs.[13−15] In principle, this approach to sizing is similar to optical methods developed by Schwartz and colleagues.[2−4] The AFM has better resolution and signal-to-noise ratio, while the light microscope has a larger bandwidth and less stringent sample requirements. In the best case, the AFM can resolve single atoms

* Address correspondence to this author. Phone: +1-410-614-3795. Fax: +1-410-614-3797. E-mail: jan.hoh@jhu.edu.

[†] Department of Physiology.

[‡] Applied Physics Laboratory.

(1) Ausubel, F. M., Brent, R., Kingston, R. E., Moore, D. D., Seidman, J. G., Smith, J. A., Struhl, K., Eds. *Current Protocols in Molecular Biology;* John Wiley & Sons: 1994; Vol. 1.
(2) Schwartz, D. C.; Li, X.; Hernandez, L. I.; Ramnarain, S. P.; Huff, E. J.; Wang, Y. K. *Science* **1993**, *262*, 110−4.
(3) Samad, A. H.; Cai, W. W.; Hu, X.; Irvin, B.; Jing, J.; Reed, J.; Meng, X.; Huang, J.; Huff, E.; Porter, B.; Shenkar, A.; Anantharaman, T.; Mishra, B.; Clarke, V.; Dimalanta, E.; Edington, J.; Hiort, C.; Rabbah, R.; Skiada, J.; Schwartz, D. C. *Nature* **1995**, *378*, 516−517.
(4) Meng, X.; Benson, K.; Chada, K.; Huff, E. J.; Schwartz, D. C. *Nat. Genet.* **1995**, *9*, 432−438.
(5) Parra, I.; Windle, B. *Nat. Genet.* **1993**, *5*, 17−21.
(6) Henry, C. *Anal. Chem.* **1997**, *69*, 243A−246A.
(7) Fitzgerald, M. C.; Zhu, L.; Smith, L. M. *Anal. Chem.* **1993**, *65*, 3204−3210.
(8) Muddiman, D. C.; Anderson, G. A.; Hofstudler, S. A.; Smith, R. D. *Anal. Chem.* **1997**, *69*, 1543−1549.
(9) Huang, Z.; Petty, J. T.; O'Quinn, B.; Longmire, J. L.; Brown, N. C.; Jett, J. H.; Keller, R. A. *Nucleic Acids Res.* **1996**, *24*, 4202−4209.
(10) Castro, A.; Fairfield, F. R.; Shera, E. B. *Anal. Chem.* **1993**, *65*, 849−852.
(11) Kasianowicz, J. J.; Brandin, E.; Branton, D.; Deamer, D. W. *Proc. Natl. Acad. Sci. U.S.A.* **1996**, *93*, 13770−13773.
(12) Binnig, G.; Quate, C. F.; Gerber, C. *Phys. Rev. Lett.* **1986**, *56*, 930−933.
(13) Hansma, H. G.; Hoh, J. H. *Annu. Rev. Biophys. Biomol. Struct.* **1994**, *23*, 115−139.
(14) Bustamante, C.; Rivetti, C. *Annu. Rev. Biophys. Biomol. Struct.* **1996**, *25*, 395−429.
(15) Shao, Z.; Mou, J.; Czajkowski, D. M.; Yang, J.; Yuan, J.-Y. *Adv. Phys.* **1996**, *45*, 1−86.

S0003-2700(97)01187-6 CCC: $15.00
Published on Web 04/02/1998

(0.2 nm resolution).[16] Under more typical imaging conditions, the resolution is 2−20 nm, which is still more than an order of magnitude better than that from optical microscopy (>200 nm). The exceptionally high signal-to-noise ratio for the AFM allows direct visualization of individual DNA or protein molecules without contrast enhancing agents.[13−15] On the other hand, optical microscopy has a substantially higher bandwidth than AFM. Optical microscopes are typically limited by video cameras to data collection rates of <10 MHz, while current AFMs are typically limited by cantilever or feedback loop performance to rates of <100 kHz. The sample requirements for optical microscopy are also somewhat less stringent than those for AFM, since the AFM sample must be sufficiently immobilized to withstand the mechanical interactions with the tip.

We are developing methods and technology for a high-throughput solid-state DNA sizing (SSDS) approach based on AFM. The general approach is to attach DNA molecules to a surface, image the molecules adsorbed on the surface, and finally determine the distribution of molecular lengths in the sample. This approach yields results comparable to those from agarose gel electrophoresis for some types of samples. Further, AFM has potential to detect directly details of DNA such as supercoiled geometries,[17] DNA kinks,[18] and varied helical repeats of single DNA molecules,[19] or to directly map proteins bound to DNA molecules,[20−23] thereby providing additional types of valuable information.

EXPERIMENTAL SECTION

DNA and Chemicals. The DNAs used were the following: low-mass DNA ladder containing equimolar amounts of 100, 200, 400, 800, 1200, and 2000 bp (Life Technologies, Gaithersburg, MD), individual ALFexpress Sizer molecules of 200, 250, or 300 bp (Pharmacia Biotech, Piscataway, NJ), 1−4.2-kb DNA ladder containing 1-, 1.5-, 2-, 2.5-, 3-, and 4.361-kb fragments (Bio-Rad Co., Hercules, CA), and 100-bp DNA ladder containing 100-, 200-, 300-, 400-, 500-, 600-, 700-, 800-, 900-, 1000-, and 1500-bp fragments (Promega, Madison, WI). The stoichiometries of the latter two mixtures are not known. DNAs were diluted with deionized water before use unless specified otherwise. Millipore-purified water (>18 MΩ cm^{-1}, MilliQ-UV, Millipore Co., Bedford, MA) was used throughout. Salts and buffers were used as received from Sigma Chemical Co. (St. Louis, MO).

PCR Amplification. All standard 35-cycle PCRs were performed in either 5- or 25-μL volumes, containing 20 pmol of each primer, 200 μM dNTPs (Perkin-Elmer Co., Norwalk, CT), 1.5 mM $MgCl_2$, 75 mM Tris-HCl (pH 9.0), 50 mM KCl, and 0.1 unit of Taq polymerase (Boehringer Mannheim, Indianapolis, IN) per microliter of reaction volume. About 2 ng of PAC template DNA was used for 25-μL reactions and 400 pg for 5-μL reactions. Fifteen-cycle PCR runs were carried out in 5 μL total volume, containing 2 pmol of primer, 35 μM dNTPs, and 0.004 unit of Taq polymerase per microliter reaction volume. Thermal cycling was carried out in a Hybaid Thermal Cycler (Hybaid Limited, Middlesex, UK). Agarose gel electrophoresis and Southern blotting were carried out using standard conditions as described elsewhere.[1]

Substrates and Sample Adsorption. Muscovite mica disks of 9 mm in diameter attached to a metal disk were used as substrates for DNA adsorption. For typical adsorption, 20 μL of a DNA solution containing 0.2−0.5 ng/μL DNA and 1 mM $MgCl_2$ was deposited onto freshly cleaved mica. The sample was incubated on the mica at room temperature for 5 min, rinsed with about 30 mL of water under flow, and blown dry with compressed air for several seconds. Variations of this procedure are described in the text.

AFM Imaging. A Nanoscope IIIa AFM controller with a multimode AFM (Digital Instruments, Santa Barbara, CA) was used for image acquisition. Single-crystal silicon cantilevers (model TESP, Digital Instruments) were cleaned by exposure to high-intensity UV light (UVO-Cleaner, Jelight Co. Inc., Laguna Hills, CA) for 3 min before use. All AFM imaging was conventional ambient tapping mode AFM,[24] with scan speeds of about 5 Hz and data collection at 512 × 512 pixels.

Automated Image Processing. Data processing was performed on a Macintosh-compatible computer (PowerTower 225, Powercomputing Co., Round Rock, TX). Automated image analysis routines were developed in the Interactive Data Language (IDL, Research Systems Inc, Boulder, CO). Further details of the image analysis routines are described below and will appear elsewhere.[25,26]

RESULTS

The approach to solid-state DNA sizing (SSDS) proposed here has three major steps: (1) the attachment of the DNA sample to a solid support, (2) AFM imaging of the sample, and (3) automated determination of length distribution from the image data (Figure 1). This parallels the use of gels in that the input to the process is a DNA sample in solution and the output is a histogram of DNA sizes in the sample. The attachment approach described here is based on adsorption from solution, which has been widely used by others.[13−15,27,28] We have initially focused on smaller fragments, typically less than 10 kb.

DNA Immobilization. We have examined a number of parameters that effect the adsorption of DNA onto mica surfaces. It is known that divalent metal ions such as Mg(II), Ca(II), Ni(II), Zn(II), and Mn(II) can be used to prompt the adsorption of

(16) Giessibl, F. J. *Science* **1995**, *267*, 68−71.
(17) Rippe, K.; Mucke, N.; Langowski, J. *Nucleic Acids Res.* **1997**, *25*, 1736−1744.
(18) Han, W. H.; Lindsay, S. M.; Dlakic, M.; Harrington, R. E. *Nature* **1997**, *386*, 563.
(19) Yang, J.; Wang, L.; Camerini-Otero, R. D. *Nanobiology* **1996**, *4*, 93−100.
(20) Rees, W. A.; Keller, R. W.; Vesenka, J. P.; Yang, G.; Bustamante, C. *Science* **1993**, *260*, 1646−1649.
(21) Allison, D. P.; Kerper, P. S.; Doktycz, M. J.; Spain, J. A.; Modrich, P.; Larimer, F. W.; Thundat, T.; Warmack, R. J. *Proc. Natl. Acad. Sci. U.S.A.* **1996**, *93*, 8826−8829.
(22) Pietrasanta, L. I.; Schaper, A.; Jovin, T. M. *Nucleic Acids Res.* **1994**, *22*, 3288−3294.
(23) Wyman, C.; Grotkopp, E.; Bustamante, C.; Nelson, H. C. M. *EMBO J.* **1995**, *14*, 117−123.
(24) Hansma, P. K.; Cleveland, J. P.; Radmacher, M.; Walters, D. A.; Hillner, P. E.; Bezanilla, M.; Fritz, M.; Vie, D.; Hansma, H. G.; Prater, C. B.; Massie, J.; Fukunaga, L.; Gurley, J.; Elings, V. *Appl. Phys. Lett.* **1994**, *64*, 1738−1740.
(25) Spisz, T. S.; D'Costa, N.; Seymour, C. K.; Hoh, J. H.; Reeves, R.; Bankman, I. N. *Proceedings of 1997 IEEE International Conference on Image Processing*, Santa Barbara, CA, 1997; Vol. 3, pp 154−157.
(26) Spisz, T. S.; Fang, Y.; Seymour, C. K.; Hoh, J. H.; Reeves, R. H.; Bankman, I. *N. Med. Biol. Eng., Comput.*, in press.
(27) Bustamante, C.; Vesenka, J.; Tang, C.; Rees, W.; Guthold, M.; Keller, R. *Biochemistry* **1992**, *31*, 22−26.
(28) Hansma, H. G.; Laney, D. E. *Biophys. J.* **1996**, *70*, 1933−39.

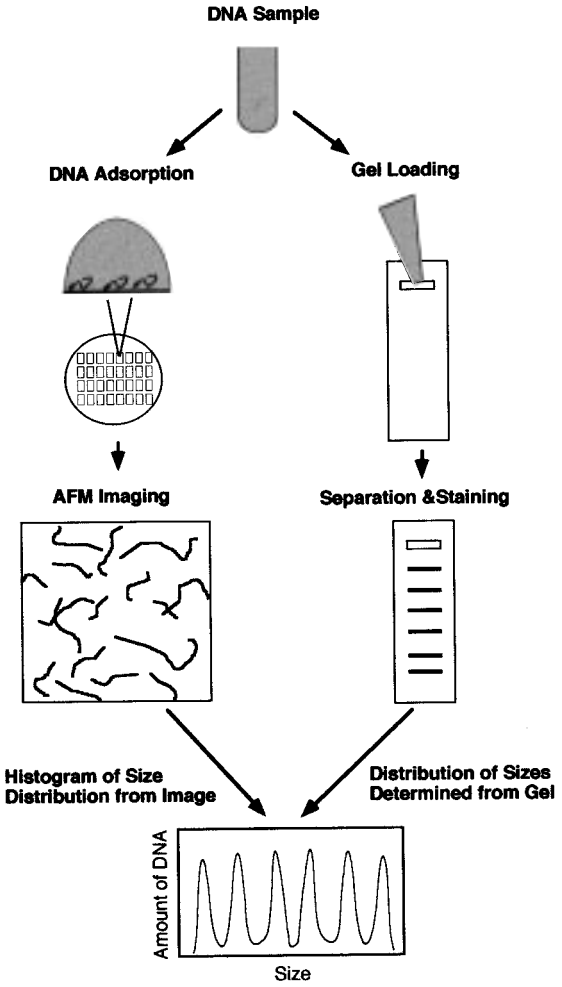

Figure 1. Scheme for solid-state DNA sizing based on AFM imaging proposed here, compared with agarose gel electrophoresis. DNA molecules are adsorbed onto a solid support (in this case, mica). The adsorbed DNA is imaged by AFM, and the fragment lengths are automatically determined using pattern recognition software. The result is a histogram of fragment lengths, which is similar to the scan of a DNA sample separated on an agarose gel.

DNA onto the mica, and the adsorption depends on the cation species.[28] In agreement with this, we find that the density of the DNA adsorbed on the mica is dependent on the concentration and species of cations used. The presence of Mg(II), Mn(II), or Ni(II) at 1 mM concentration gives rise to similar densities of DNA molecules on the mica, whereas both Zn(II) and Ca(II) prompt fewer DNA molecules onto the mica (Table 1).

The cation type was also found to affect the measured length of DNA fragments, with Ca(II) producing a significant shortening of the molecules. The average contour lengths of 250-bp DNA fragments adsorbed on the mica using different types of cations were determined using the automated sizing program described below. For B-form DNA, this fragment should be 84.2 nm. However, the mean contour length varied significantly with the cationic species (Table 1). The DNA fragments are more extended in the presence of both Mg(II) and Mn(II) than those in the presence of Zn(II) and Ni(II), while Ca(II) yields the shortest mean contour length (Figure 2). The concentration of Mg(II) in the range of 0.5−10 mM did not obviously affect the measured length of the DNA at suitable incubation times.

Table 1. Cation-Dependent Contour Lengths of a 250-bp DNA[a]

cation	μ (nm)	σ (nm)	n
Mn(II)	86	6.5	1090
Mg(II)	76	7.1	1125
Ni(II)	71	8.5	1405
Zn(II)	75	8.5	532
Ca(II)	54	8.7	679

[a]Adsorption condition: 1.2 nM concentration of the 250-bp DNA and 1 mM cation. The mean contour length, μ, and the standard deviation, σ, of the DNA fragments were measured by Gaussian fitting of the length distribution using the AFMIPS software. The total DNA number presented here, n, was automatically calculated by the software from these AFM images of $2 \times 2\ \mu m^2$ obtained at five random positions of the mica surface.

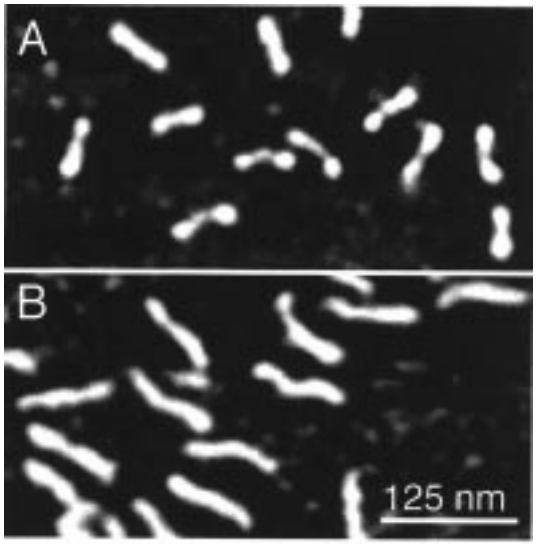

Figure 2. DNA molecules adsorbed on mica have different measured lengths in the presence of different cations. (A) Ca(II) results in obviously bending and some folding of the DNA molecules and produces measured lengths that are shorter than expected. (B) Mn(II) produces the most extend DNA fragments.

The DNA adsorption kinetics were investigated for several fragments of a single size and mixtures and were found to depend primarily on DNA fragment size and concentration. The adsorption of DNA molecules of a single size onto mica appears to be diffusion limited (Figure 3a), in agreement with previous observations.[14] The adsorption kinetics is faster for smaller molecules; hence, there is a bias for smaller DNAs that is evident in the size histograms from DNA markers (Figure 3b). The relationship between DNA size and number of fragments adsorbed to the surface is roughly exponential. It should be noted that the analysis software ignores any fragments that are touching the edge of the image or cross each other, and this would likely impose an additional bias against longer fragments in the length distribution. Finally, for different concentrations of DNA samples, the relationship between adsorption time and the number of DNA fragments adsorbed onto the surface allows appropriate incubation times to be determined (Figure 3c).

AFM Imaging. All AFM images were 512 × 512 pixels, but the size of the area imaged was selected on the basis of the size of the DNA fragments. For small DNA fragments of 100−500 bp, an image size of 1−2 μm, which is 2−4 nm/pixel, produces

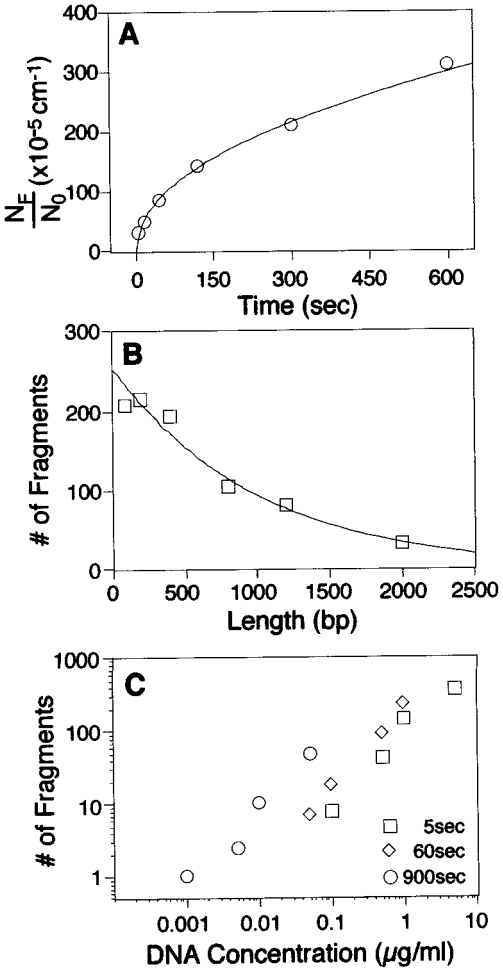

Figure 3. Adsorption kinetics of DNA fragments onto a mica surface in the presence of $MgCl_2$ at room temperature. (A) Adsorption kinetics of the 250-bp sizer in the presence of 1 mM $MgCl_2$, where a 20-μL drop of 1 nM DNA solution was incubated on mica for a certain time and rinsed with water to stop the DNA adsorption. N_F is the number of DNA fragments per square centimeter adsorbed on the surface, measured from six 2 × 2 μm^2 images, and N_0 is the total number of molecules per cubic centimeter of the DNA solution. (B) Size dependence of the adsorption kinetics results in a bias toward smaller fragments. This is opposite what typically happens in gel electrophoresis, where the intensity depends on the mass of DNA, which, for equimolar samples, falls with decreasing size. Here, the low-mass DNA ladder was used. Ten AFM images of 2 × 2 μm^2 were subject to statistical analysis. (C) The adsorption of DNA to the surface also depends on DNA concentration. Varying both time and concentration shows that, for concentrated samples, the time to achieve adequate adsorption is on the order of seconds. For these experiments, raw 300-bp PCR product was diluted to different concentration in 10 mM $MgCl_2$.

optimal results (Figure 4). Scan sizes larger than 2 μm produce pixel sizes that reduce the precision of measurements. Acquisition time is approximately 2 min/image. The minimum image acquisition time has not been evaluated here, because there are a number of technological improvements being pursued elsewhere that should significantly improve speed. We have also collected preliminary images with a custom data collection system that allows pixel densities in x and y to be specified independently. These images clearly show small DNA fragments in an 8192 × 8192 pixel image over a 20 × 20 μm^2 area (not shown).

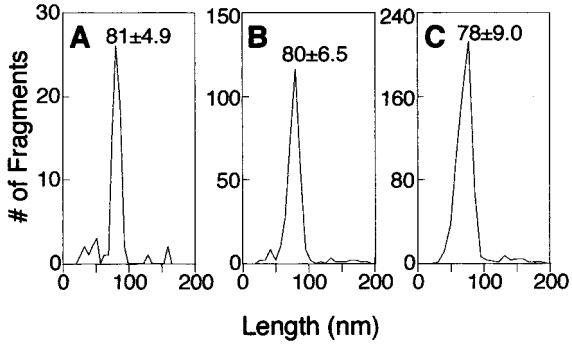

Figure 4. Dependence of the measured contour length of the 250-bp DNA sizer on the image scan size. (A) The smaller scan sizes (1 × 1 μm^2) have tighter distributions (i.e., better precision). (B,C) The larger scan sizes (2 × 2 μm^2 and 3 × 3 μm^2) have broader distributions. These differences probably result from different pixel sizes (all images are 512 × 512), which are 1.95, 3.90, and 5.86 nm for (A), (B), and (C), respectively.

Automatic Sizing Software. To rapidly and accurately determine the distribution of DNA lengths in the AFM images, we have developed specialized software (called AFMIPS) written in the Interactive Data Language (IDL). IDL is a high-level interactive programming environment that is designed to handle and manipulate large arrays of data. The software is platform independent and has a user-friendly graphical interface. It also provides a wide array of advanced processing tools and allows for rapid modification and upgrade of the software. The drawback of using IDL is that it is slower than typical compiled computer languages such as C. However, the processing time per image is still <60 s, which allows more than 1500 images/day to be processed on an inexpensive personal computer.

The present version of the analysis software uses an AFM image of DNA adsorbed onto a substrate as input and follows a series of conventional image processing steps (Figure 5). The end result is a histogram of sizes similar to a scan of gel-separated DNAs. The most critical data parameters for this software are that the background is kept to a reasonable level and the density of fragments is not so high that there are frequent overlaps. Program performance is primarily validated by comparison with hand-traced results using NIH Image software (Figure 6). These comparisons show that the precision of the program is comparable to hand tracing, although in some cases the two approaches produce slight differences in the average lengths. This indicates some systematic difference between the two, which likely arises from the way in which the person hand tracing determines the end points of the molecule. Full details of the program will be presented elsewhere.[25,26]

Performance. Using single samples prepared, imaged, and processed (with AFMIPS) manually, the accuracy, precision, resolution, and sensitivity of the SSDS for PCR products and small DNA fragments were evaluated. The accuracy is determined by subjecting a series of DNA samples with known size to SSDS. Typically, the measured length was within 15% of the expected length, based on the known size. The precision of the SSDS was assessed by the width of a distribution peak at half-height. This value was typically <10% of the fragment length, for fragments >200 bp. Precision does not improve significantly for hand tracing of DNA contours (Figure 6), suggesting that it is limited by sample

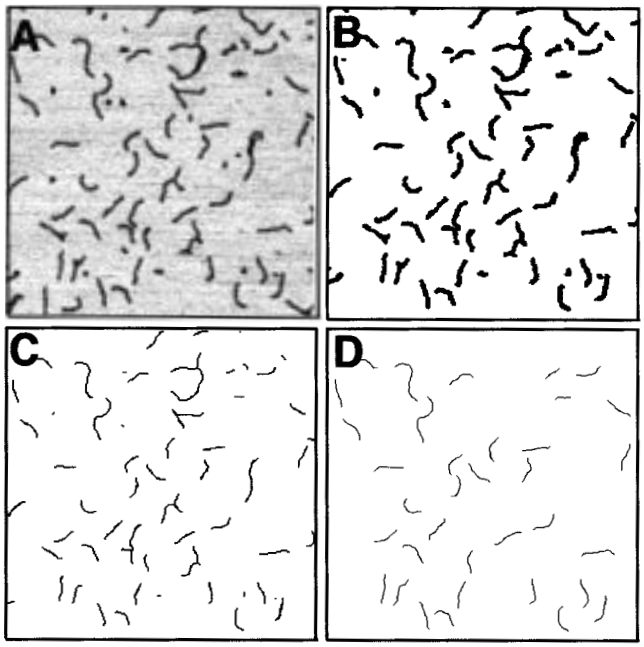

Figure 5. Examples of intermediates in the automated DNA sizing process using AFMIPS. (A) AFM image (contrast inverted). (B) After thresholding based on the optimum threshold obtained by Gaussian fitting, both foreground and background gray scale data,[29] and followed by smoothing the binary image with a 3 × 3 pixel average. (C) After pruning and thinning by using a fast parallel thinning algorithm, in which the pixels are removed only if a set of conditions for the pixel's neighborhood are met, until no further pixels satisfy the conditions for removal.[30] (D) After removing these overlapping fragments with more than two end points and edge-touching fragments.

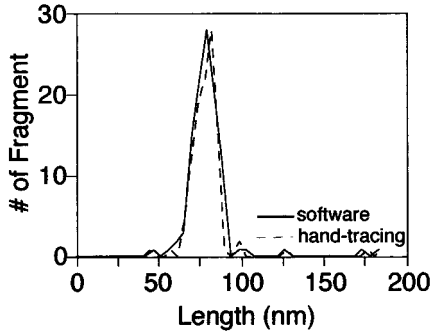

Figure 6. Comparison of automated size analysis with hand tracing of the same images of the 250-bp sizer.

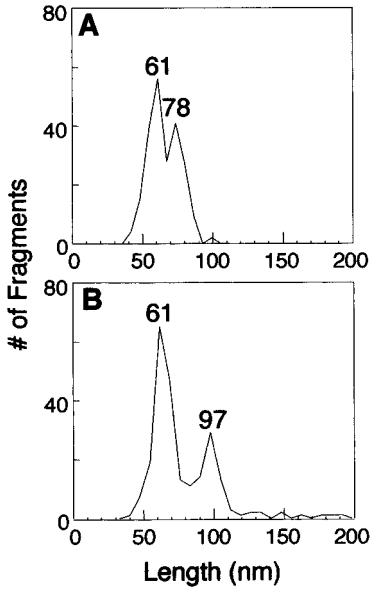

Figure 7. Empirical evaluation of the resolution of SSDS using mixed size samples. (A) An equimolar mixture of 200-bp and 250-bp DNAs shows two resolved peaks, as does (B) an equimolar mixture of 200-bp and 300-bp DNAs.

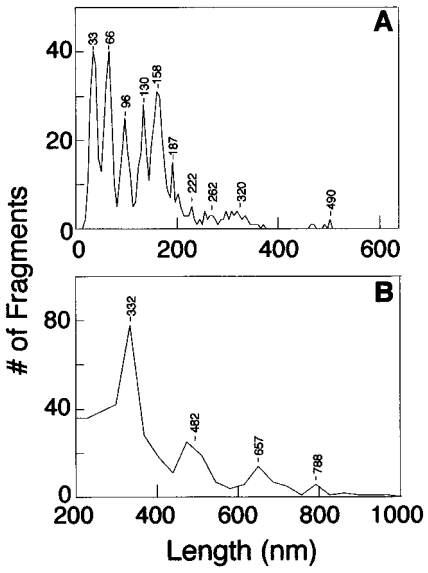

Figure 8. Length distribution of two common DNA markers, determined by SSDS. (A) A 100-bp DNA ladder and (B) a 1−4.2-kb DNA ladder.

preparation or image acquisition. The precision also gives one measurement of the resolution. A more practical assessment of resolution is provided by examining known mixtures of DNA fragments. These experiments show that a 200-bp fragment can be distinguished from a 250-bp fragment (Figure 7). Furthermore, the lower molecular weight fragments of both the 100-bp DNA ladder and the 1−4.1-kb DNA ladder can be easily separated from the histograms of the size distribution (Figure 8). The longer DNA fragments in these DNA ladders are less well represented, due to the relatively slow adsorption kinetics.

In principle, the AFM has single molecule sensitivity in DNA sizing experiments, since a single molecule attached to a surface provides sufficient signal-to-noise ratio in the imaging process to produce an image that reflects the length of the DNA. At present, however, it is not possible to recover and locate a single DNA fragment for analysis. A serial dilution experiment shows that a practical concentration limit for the sample preparation is near 10 pg/μL (Figure 3c). The volume in these experiments was 5 μL, which covered ~1 cm^2 on the mica. The area covered is many orders of magnitude larger than needed, and if the sample volume is adjusted to cover 1 mm^2, the lower detection limit will be <500 fg for a 300 bp DNA (~3 amol).

Test Application. SSDS was tested in a blind comparison with agarose gel electrophoresis for +/− screening of a set of P1 artificial chromosomes (PACs). A PAC set was generated by screening a PAC library (BAC PAC Resources, Roswell Park Cancer Institute). A single YAC of 350 kb was isolated from a pulsed field gel, radioactively labeled, and hybridized to PAC

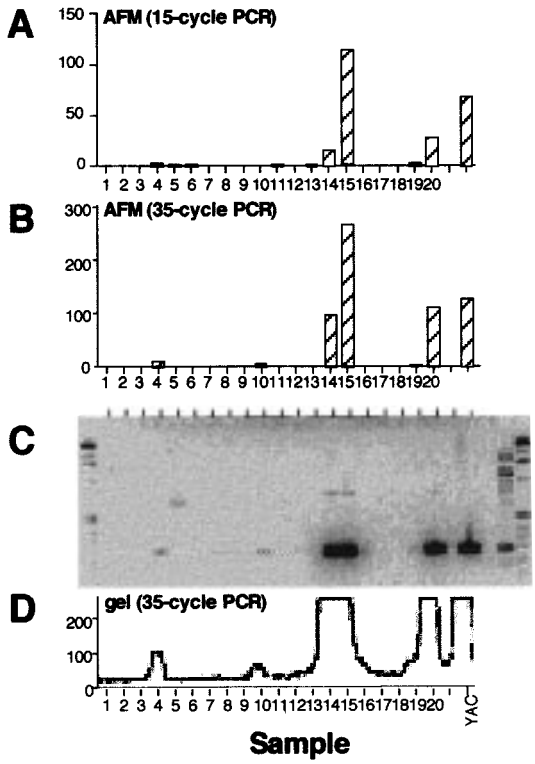

Figure 9. Comparison of SSDS with agarose gel electrophoresis for ± screening. The SSDS results using the 15-cycle or 35-cycle PCR reactions are in excellent agreement with the agarose gels run using the 35-cycle reactions. AFM images of 3 × 3 μm^2 areas for each sample were obtained from randomly selected areas (samples are numbered 1−20). Using the AFMIPS software, fragments within a 30-nm window of expected value were counted. (A) The 15-cycle PCR reactions showed a distribution of fragments very similar to (B) the 35-cycle reactions. (C). Agarose gels of the same samples gels were run and (D) optically scanned along the line of the expected 370-bp PCR product (white dashed line). The distribution of the 370-bp fragment in the densitometric scan was in excellent agreement with the SSDS data.

library filters. The resulting set of 20 positive clones were screened for the presence of known markers on the YAC, using PAC DNAs as template for either 15- or 35-cycle PCR reactions. The same set of PCR products was examined by SSDS.

For gel electrophoresis, products of the 15- and 35-cycle reactions were separated in agarose, and the resulting gels were stained with SYBR Green (Molecular Probes). The 15-cycle reaction could not be reliably detected by UV visualization of the stained gel but were detected by hybridization of radioactively labeled PCR product to a Southern blot of the gel (data not shown). Aliquots of the same samples were assessed by SSDS. Products of the 20-μL, 35-cycle reactions were diluted 1:10 before adsorption onto mica, while 2 μL of the product from the 5-μL, 15-cycle reaction was used directly. The results from SSDS were in excellent agreement with the gel-based results (Figure 9).

The error rate in SSDS remains to be formally established, although we estimate the present failure/error rate to be between 0.01 and 0.001. Errors typically occur when the sample preparation fails in some way, such that there is no sample on the substrates. The time required to perform SSDS is, at present, several minutes per sample. In one set of experiments, manual processing of 60 PCR samples by one individual was completed in approximately 4 h. Many steps of this process are amenable to automation, which should provide rapid throughput (discussed below).

DISCUSSION

DNA can be attached to a surface and imaged with an AFM, and the contour length of the DNA in the resulting image reflects the number of base pairs in the DNA.[13−15,21,31−34] We examined several parameters of this process to determine whether this method for sizing DNA might be useful or better than other approaches, particularly gel electrophoresis. The results presented here suggest that SSDS is a promising approach for certain applications for several reasons, including the speed of individual analyses, sensitivity, potential for automation, and reduced PCR reaction sizes.

One important feature of SSDS is that sizing a single sample is very fast compared to gels. A gel takes 1−2 h to separate, whether there is one sample or 30 on it, while a single DNA sample can be manually prepared and sized by SSDS in <10 min (likely much less than that in the future). In situations when speed is critical, e.g., evaluation of pathological samples during surgery, the ability to provide rapid results outweighs other considerations. The speed of SSDS analyses of PCR reactions is also improved by the high sensitivity of the method, which allows the number of PCR cycles needed to generate adequate amplification to be reduced significantly. It is important to note that PCR reactions can be used directly, without any purification or manipulation other than adsorption to a surface.

The SSDS method described here is well-suited to analysis of PCR reactions and provides specific advantages deriving from the sensitivity and signal-to-noise properties. Because <50 DNA molecules need to be measured to produce a useful histogram, reactions can be scaled back not only in time but also in volume, which saves on costly reagents. In the test application performed here, reagent cost was reduced to <25% that of a standard PCR reaction. It is likely that further optimization of parameters for reactions of smaller scale and shorter cycles can be accomplished. Unlike gel electrophoresis, which requires the addition of loading dyes following PCR, SSDS allows samples to be analyzed directly from the PCR reaction mixture. Gels also require staining and image acquisition if run manually, and the required manipulations of the gel make this difficult to automate. The problem is circumvented if fluorescent-labeled PCR primers are used and the reactions are analyzed in an automated DNA sequencer; the reagent cost for these reactions is substantially greater, and they have not proven amenable to reduced volume/cycle times.

The proposed SSDS system will become more useful if it can be highly automated. Considering the three steps of the process, the sample preparation is, at present, the most difficult to automate. Automated pipetting can be employed to deposit

(29) Gonzalez, R. C.; Wintz, P. *Digital Image Processing*; Addison-Wesley Publishing Co.: Reading, MA, 1987.
(30) Zhang, T. Y.; Suen, C. Y. *Commun. ACM* **1984**, *27*, 236−239.
(31) Rivetti, C.; Guthold, M.; Bustamante, C. *J. Mol. Biol.* **1996**, *264*, 919−932.
(32) Coury, J. E.; Anderson, J. R.; Mcfail-Isom, L.; Williams, L. D.; Bottomley, L. A. *J. Am. Chem. Soc.* **1997**, *119*, 3792−3796.
(33) Lyubchenko, Y.; Shlyakhtenko, L.; Harrington, R.; Oden, P.; Lindsay, S. *Proc. Natl. Acad. Sci. U.S.A.* **1993**, *90*, 2137−2140.
(34) Hansma, H. G.; Browne, K. A.; Bezanilla, M.; Bruice, T. C. *Biochemistry* **1994**, *33*, 8436−8441.

sample onto surfaces, and procedures to spot 25 samples/cm^2 are routine. The size of the sample "spots" in these arrays greatly exceeds that required for SSDS. We are exploring deposition methods specifically designed for AFM samples that should allow for much higher density spotting. Automated imaging is well established for AFMs used in semiconductor quality control. These systems utilize AFMs that run 24 h/day with automated sample exchange, tip positioning (to better than 1 μm accuracy), tip exchange, and data validation. The data analysis software we have developed can readily be integrated with automated sample collection, such that analysis occurs immediately after data collection and without operator intervention. Hence, SSDS can be highly automated for high-throughput applications.

In addition to the +/− screening and sizing applications discussed here, AFM can be used to visualize DNA molecules that have been allowed to interact with proteins, in which the proteins recognize specific short stretches of sequence within the DNA molecule, such as restriction enzymes.[14,21,35] By directly visualizing the position of the binding proteins, the distance between the binding sites can be determined, and the order of the fragments is maintained. This is a significant advantage over gel electrophoresis of restriction digests, where the order of fragments is lost. More generally, the AFM can be used to examine DNA that has been "decorated" in any sequence-dependent manner that produces contrast. For example, hybridization of short oligomers to create triple helical regions that can be readily visualized by AFM, as can some chemical modifications (unpublished observation), and the binding of sequence specific proteins. This could be used as a type of "bar-coding" of DNA with many potential health care and forensic applications, where complete sequence is not needed but sizes of restriction fragments alone is inadequate.

(35) Niu, L.; Shaiu, W. L.; Vesenka, J.; Larson, D. D.; Henderson, E. *Proc. SPIE-Int. Soc. Opt. Eng.* **1993**, *1891*, 71−77.

CONCLUSION

The conditions for SSDS established here provide a basis for development of highly automated, high-throughput assessment of many types of samples with a wide variety of applications in research and health care. The potential for reduced reaction times and reagent costs, and the available procedures for automation suggests that SSDS represents a competitive process with potential applications in many types of DNA analysis.

ACKNOWLEDGMENT

This work was supported by NIH Grants HGO1518-02 (J.H.H.) and HGO095-07 (R.H.R.) and internal research and development funds from the Johns Hopkins University Applied Physics Laboratory (T.S.S. and I.N.B.). We thank Shawn Lupold, Damon Brown, and Cheryl Seymour for assistance.

Received for review October 24, 1997. Accepted February 24, 1998.

AC971187O